Microwave Permittivity of Dry Sand

Christian Mätzler

***Abstract*—The complex, relative dielectric permittivity ε of dry desert sand, collected at the Grand Erg Oriental in Ksar Ghilane, Tunisia, in October 1994, was measured with microwave resonators at frequencies between 0.245 and 6 GHz. The results are presented here. Whereas the real part ε' is nearly independent of frequency, a monotonous decrease of the imaginary part ε'' with increasing frequency is observed. The data can be fitted to a Debye relaxation spectrum with a relaxation frequency of about 0.27 GHz, leading to a nearly frequency-independent penetration depth of about 1 m over the range from 1–10 GHz. The spectrum can be explained by Maxwell–Wagner losses of semiconducting spheres embedded in a nonconducting sand medium.**

I. Introduction and Sample Description

Interest in the microwave dielectric properties of natural materials occurring at the earth's surface is based on potential applications in active and passive microwave remote sensing. Speculation about seeing underground features in L-Band radar images of arid regions has appeared in the literature, assuming sufficiently deep penetration of the sensing waves. Knowledge of the penetration depth is also required in passive microwave remote sensing to estimate the effective emission temperature in case of a temperature gradient within the emitting layer on the one hand and for modeling volume scattering on the other. Quantitative information of the electromagnetic properties of arid surfaces over a broad frequency range is largely missing. The present contribution helps to fill this gap. Dry desert sand, collected in October 1994 in a large desert of the Sahara, i.e., of the Grand Erg Oriental in Ksar Ghilane, Tunisia, was investigated. The sand is fine grained, and its color is a bright red-brown, typical for the region. The 1.5 l sample was kept in a gas-tight plastic bottle until the dielectric measurements were made in the laboratory in November 1994. The liquid-water content was below 0.2% by weight, i.e., low enough to be negligible in the present data. It is supposed that the sample is representative for the whole area, since sand is very mobile and, thus, well mixed.

II. Sensors

The dielectric measurements were made with two resonators. At frequencies below 1 GHz, an open-ended coaxial resonator (with a diameter of 7 cm and length of 20 cm) made from stainless steel was used. It was developed for measurements of snow [2], [4]. At higher frequencies, a gilded-copper rectangular microwave cavity (with side lengths of 5, 6.5, and 8 cm) operating in different modes was developed by Wegmüller [7], who used it for ice dielectric measurements [3]. The measurements were made by completely filling the resonators with sand. Both resonators were operated in transmission by using a network analyzer. The data analysis was done according to the method described by Mätzler and Wegmüller [3].

III. Results

For harmonic time (t)-dependence of the form $e^{-i2\pi ft}$, the spectra of the dielectric sand data at room temperature (22° C) are shown in Fig. 1, together with the density and with the fitted curves discussed below. The real permittivity is fairly constant, showing only a slight tendency toward decreasing values with increasing frequency. The values near $\varepsilon' = 2.6$ are typical for dry sand [6]. On the other hand, the imaginary permittivity shows a strong decrease, starting with 0.13 at $f = 0.25$ GHz and reaching values as low as 0.012 near 6 GHz. For the modeling of the data, a Debye relaxation spectrum is chosen. A physical explanation for such a spectrum can be given by Maxwell–Wagner losses as a result of a conducting or semiconducting component included in a mainly nonconducting sand-particle mixture (see the Appendix for an estimate of this situation). The imaginary part of (1)

$$\varepsilon = \varepsilon' + i\varepsilon'' = \varepsilon_\infty = (\varepsilon_s - \varepsilon_\infty)/(1 - if/f_0) + ia'' \qquad (1)$$

was fitted to the data points of ε'', where $i = \sqrt{-1}$. The following parameters resulted with an R^2 of 0.98: $\varepsilon_s - \varepsilon_\infty = 0.26$, $f_0 = 0.27$ GHz, and $a'' = 0.002$ is an estimated imaginary part assumed to be due to losses of the main sand component. The standard deviation of the fit is 0.0058 for ε'', and the real part of the fit follows the data points quite well if we choose $\varepsilon_\infty = 2.53$, resulting in $\varepsilon_s = 2.79$. For this fit, any influence by the slightly variable density has been neglected. The sand density only slightly changed with increasing pressure; obviously the sand was densely packed by its own gravity. The data should have been extended by measurements at lower frequencies in order to validate the maximum of ε'' predicted by the model. Unfortunately, the selected resonators were too small to allow such an extension.

A comparison with dielectric data of a quartz-dominated beach sand from the Western United States [5] shows a qualitative agreement with the data of Fig. 1 over the frequency range from 0.3–3 GHz (water content 0.3% by volume). The increase of ε'' with decreasing frequency was also identified, while the change with frequency, however, was smaller.

IV. Penetration Depth

The power penetration depth p is given by the inverse of the absorption coefficient α, which is $\alpha = 2k_0 n''$, where k_0 is the wave number in vacuum and n'' is the imaginary part of the complex refractive index $n = \sqrt{\varepsilon}$. In (1), p was computed over the frequency range from 0.1–10 GHz. The result is shown in a logarithmic representation in Fig. 2. The main feature derivable from the presented dielectric data is the plateau region at $f \geq 1$ GHz. This plateau results from the high-frequency tail of the Debye spectrum. The higher values at the very low frequencies are less accurate, and the decrease at frequencies above $\cong 6$ GHz is not very reliable, since it depends on the behavior of a''.

V. Conclusions

The complex permittivity $\varepsilon = \varepsilon' + i\varepsilon''$ of sand is the key parameter for electromagnetic wave propagation. Here we presented experimental data of the spectral behavior of ε in the range from 0.245–6 GHz by using dry Sahara sand. A characteristic frequency dependence of ε'' was discovered. The data are consistent with a Debye relaxation spectrum with a relaxation frequency of 0.27 GHz. A consequence of this result is a constant penetration depth of about 1 m extending over a large frequency range (1–10 GHz). At higher frequencies, a decrease of p was estimated from the parameter a'', whose actual behavior is uncertain due to missing measurements. The penetration of microwaves into this sand is thus quite large, many wavelengths. The consequences are that volume scattering by inhomogeneities within the sand may be significant for remote

Manuscript received November 20, 1996; revised April 9, 1997. This work was supported by ESA Study AO/3019/95/NL/NB, "Retrieval of geophysical parameters with integrated modeling of land surfaces and atmosphere."

The author was with the Polar Science Center of the Applied Physics Laboratory, University of Washington, Seattle, WA 98195 USA. The author is now with the Institute of Applied Physics, University of Bern, CH-3012 Bern, Switzerland (e-mail: matzler@iap.unibe.ch).

Publisher Item Identifier S 0196-2892(98)00138-7.

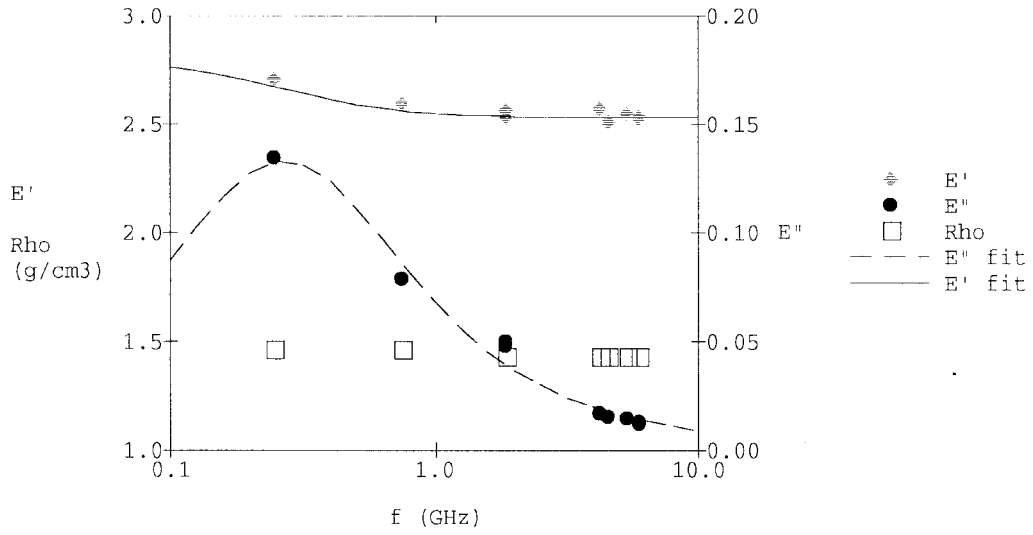

Fig. 1. Measured real (diamonds) and imaginary (circles) parts of the relative permittivity of sand versus frequency. Also shown is the density (squares), Rho, of the sand for the respective measurements. The solid and dashed curves are a fitted spectrum according to (1) with the following parameters: $\varepsilon_s = 2.79, \varepsilon_\infty = 2.53, f_0 = 0.27$ GHz, $a'' = 0.002$.

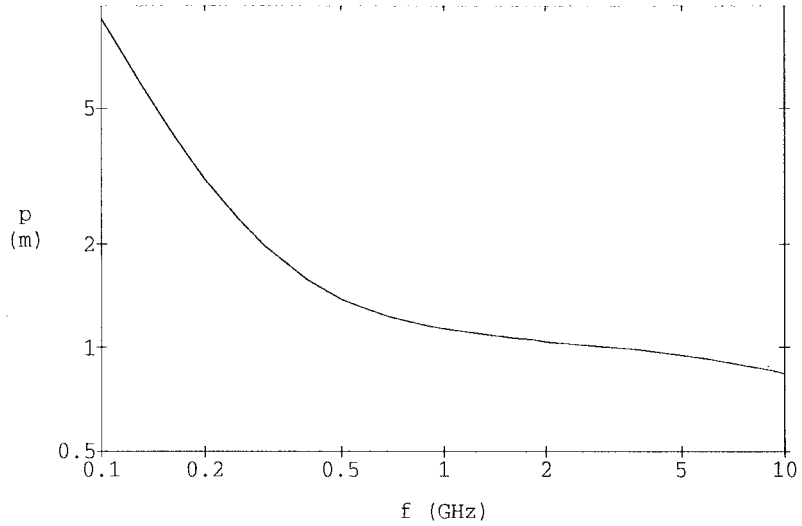

Fig. 2. Penetration depth of sand versus frequency, according to the fitted permittivity.

sensing and that the effective emission temperature (approximately the temperature at the depth p below the surface) can be much different from the surface temperature.

An open question is the origin of the Debye spectrum. According to the results of the Appendix, the Debye spectrum can be explained by a conductive component of the sand, consisting of spherical particles with a volumetric-fill factor near 0.05 and a conductivity between 0.1 and 0.2 $(\Omega\mathrm{m})^{-1}$. This value is typical for a semiconducting material. Hematite $(\mathrm{Fe_2O_3})$, the typical iron mineral responsible for the reddish color of the Sahara sand, is known to have an average conductivity of 0.1 $(\Omega\mathrm{m})^{-1}$; see Keller [1]. It should be realized that sand without the Debye losses (e.g., pure quartz sand) would have a still larger penetration depth, and, consequently, the volume effects on microwave remote sensing would even be larger.

Appendix
Maxwell–Wagner Losses of Conducting Spheres in a Nonconducting Background Medium

Let us assume small, conducting spheres with conductivity σ uniformly embedded in a background medium, in our case, the main sand component with a real relative permittivity ε_1 (i.e., we neglect the small term a''). If the volume fraction v of the spheres is sufficiently small (higher order terms of v being neglected), the effective dielectric permittivity ε of the mixture is given by (see [2, Section II.B])

$$\varepsilon = \varepsilon_1 + (\varepsilon_2 - \varepsilon_1) v K \tag{A1}$$

where K is the ratio of the electrical-field strength in the sphere to the one in the main sand component, i.e.,

$$K = 3/(2 + \varepsilon_2/\varepsilon_1). \tag{A2}$$

Now the relative permittivity ε_2 of the sphere can be represented by

$$\varepsilon_2 = b + i\frac{\sigma}{\varepsilon_0 2\pi f} \tag{A3}$$

where b is the constant real part of ε_2, and ε_0 is the vacuum dielectric constant. Inserting (A3) into (A2) and (A1) leads to a Debye relaxation spectrum for ε, namely

$$\varepsilon = \varepsilon' + i\varepsilon'' = \varepsilon_\infty + (\varepsilon_s - \varepsilon_\infty)/(1 - if/f_0) \tag{A4}$$

where

$$\varepsilon_\infty = \varepsilon_1 + v\frac{3(b-\varepsilon_1)}{2+b/\varepsilon_1} \cong \varepsilon_1 \tag{A5}$$

$$\varepsilon_s - \varepsilon_\infty = v\frac{9\varepsilon_1}{2+b/\varepsilon_1} \tag{A6}$$

and

$$f_0 = \frac{\sigma}{\varepsilon_0 2\pi(2\varepsilon_1+b)}. \tag{A7}$$

Taking the parameters found for the sand and assuming $b = 4$, we get the following parameters for the conducting component: $v = 0.04$ and $\sigma = 0.13\ (\Omega\mathrm{m})^{-1}$, whereas for $b = 7.5$, we get $v = 0.06$ and $\sigma = 0.19\ (\Omega\mathrm{m})^{-1}$.

ACKNOWLEDGMENT

This paper was written while the author was a visiting scientist at the Polar Science Center of the Applied Physics Laboratory, University of Washington, Seattle. Their hospitality is acknowledged.

REFERENCES

[1] G. V. Keller, "Electrical properties of rocks and minerals," in S. P. Clark, Ed. "Handbook of physical constants," *Geolog. Soc. Amer., Memoir 97*, 1966, pp. 553–577.
[2] C. Mätzler, "Applications of the interaction of microwaves with the natural snow cover," *Remote Sens. Rev.*, vol. 2, pp. 259–392, 1987.
[3] C. Mätzler and U. Wegmüller, "Dielectric properties of freshwater ice at microwave frequencies," *J. Phys. D, Appl. Phys.*, vol. 20, p. 1623–1630, 1987; Errata, vol. 21, p. 1660, 1988.
[4] C. Mätzler, "Microwave permittivity of dry snow," *IEEE Trans. Geosci. Remote Sensing*, vol. 34, pp. 573–581, 1996.
[5] E. Njoku and J. A. Kong, "Theory for passive microwave remote sensing of near-surface soil moisture," *J. Geophys. Res.*, vol. 82, pp. 3108–3118, 1977.
[6] F. T. Ulaby, R. K. Moore, and A. K. Fung, *Microwave Remote Sensing, Active and Passive*, vol. 3. Dedham, MA: Artech House, 1986.
[7] U. Wegmüller, Diploma thesis, Inst. Appl. Phys., Univ. Bern, Switzerland, 1986.

Characterizations of Temporal Variations in Atmospheric Water Vapor

Per O. J. Jarlemark and Gunnar Elgered

***Abstract*—Microwave radiometer measurements of temporal variations in the amount of atmospheric water vapor are characterized by using "structure functions." The power-law indexes of the functions for time lags in the range 1–8 h are approximately 1.0, while a model predicts the value 2/3.**

I. INTRODUCTION

A microwave radiometer at the Onsala Space Observatory observes the sky emission at 21.0 and 31.4 GHz. It has primarily been utilized in the retrieval of the excess radio-path length, due to water vapor: the "wet delay." The retrieved wet delay can then be used for correcting space geodetic techniques, such as very-long-baseline interferometry (VLBI) [1]–[3] and the global positioning system (GPS) [4], [5]. When no independent measurement of the wet delay is at hand, it can be derived from the space geodetic data themselves aided by statistical descriptions of the expected wet-delay variation. Examples of the use of Kalman filtering in geodetic VLBI can be found in [6]. It has also been demonstrated that the wet delay derived from GPS data can have even subcentimeter accuracy [3] and can thus be used as a probe of the amount of atmospheric water vapor. With the goal to improve the accuracy of the estimated quantities in the space geodetic techniques, there will be a need for more reliable models of the wet-delay variations.

Temporal and spatial wet-delay variations derived from different measurement techniques have been compiled for a wide range of distances and time lags [7]. There is, however, a lack of temporal measurements in the region 10^2 to 10^5 s; a range relevant for the models used in space geodesy. The aim of the radiometric measurements presented in this paper is to contribute in the coverage of this shortage. We present radiometer data, derive structure functions, and discuss the error sources.

Manuscript received March 11, 1996; revised January 8, 1997. This work was supported by the Swedish Natural Science Research Council (NFR). Weather maps were supplied by the Swedish Meteorological and Hydrological Institute (SMHI).

The authors are with the Department of Radio and Space Science, Onsala Space Observatory, Chalmers University of Technology, S-43992 Onsala, Sweden (e-mail: poj@oso.chalmers.se).

Publisher Item Identifier S 0196-2892(98)00152-1.

II. MEASUREMENTS AND DATA ANALYSIS

The design and performance of the radiometer used in this study are given in [8]. There are, however, a couple of changes made since then, for instance, an A/D converter with improved resolution (corresponding to 0.015 K instead of 0.3 K), new hot reference loads, and an increase in the slewing speed from 2°/s to approximately 8°/s.

Here we present ten data sets of radiometric measurements conducted in 1988, 1992, and 1993. The duration of the measurements varies between two and eight days, yielding a total of approximately 42 days. In each data set, we used only observations acquired in one direction. The elevation angle was 30° in all ten data sets, but the azimuth angle differed between the sets. We picked four data sets from the spring and summer 1988, which contained both cloudy and cloud-free periods, and data were taken approximately every 20 s. In the data from 1992 to 1993, mainly acquired in the summer, a sampling period of either 90 or 60 s was used. The equivalent zenith wet delay was calculated from the sky brightness-temperature measurements [9]. In Fig. 1, we present the wet delay from three of the data sets.

The wet delay is of course closely related to the amount of precipitable water vapor. The wet delay is approximately a factor 6.3 times larger than the precipitable water vapor in the Swedish west coast climate (both in units of length). This factor depends on the mean temperature of the water vapor containing part of the atmosphere, and it has thus a typical seasonal variation of about ±5% in temperate climate. The results presented below is thus expected to be qualitatively valid also for the precipitable water vapor.

We have used structure functions for the characterization of the wet delay. The temporal structure function D_l of the wet delay l can be defined as

$$D_l(\tau) \stackrel{\mathrm{def}}{=} < [l(t+\tau) - l(t)]^2 > \tag{1}$$

where τ is the time lag under consideration. When using (1) in our calculations, the expectation value, indicated by $<>$, was replaced by computing the average value using all time epochs t in the data set. For a given time lag τ, the value of $D_l(\tau)$ is not influenced by variations of much longer time scales than τ [11].

Before calculating the structure functions, we removed the data where the cloud liquid content estimated from the sky brightness